FRACTURE PROCESS ZONE DEVELOPMENT IN A MAGNESIA AND A MAGNESIA SPINEL REFRACTORY AS OBSERVED BY DIGITAL IMAGE CORRELATION

Dietmar Gruber[1], Yajie Dai[2], Harald Harmuth[1]

[1]Chair of Ceramics, Montanuniversitaet, Leoben, Austria
[2]The State Key Laboratory of Refractories and Metallurgy, Wuhan University of Science and Technology, Wuhan, China

ABSTRACT

Magnesia and magnesia spinel refractories show a completely different fracture behavior. A typical magnesia spinel material and a magnesia material were selected to investigate the development of the fracture process. A wedge splitting test was applied for the fracture-mechanical test. During the test, strains as well as the crack propagation were detected by digital image correlation. Afterwards fracture mechanical data were determined from the load-displacement curves.

The mechanical properties indicate a reduction in strength and an increase in fracture energy for the magnesia spinel material. The microstructure characterized by pre-existing micro-cracks increases the strain bearing capacity, which is very important for improving the thermal shock resistance. For pure magnesia, no pronounced fracture process zone could be detected by digital image correlation. For magnesia spinel, the development of the fracture process zone starts in the pre-peak region. The fracture process of magnesia spinel is characterized by the development of the fracture process zone and the subsequent development of the macro-crack. The transition is indicated by a change of the fracture process zone width. The onset of the macro-crack is in the post-peak region when the load has already decreased to 66% of its maximum value.

KEYWORDS

Magnesia refractories, fracture process zone, digital image correlation, wedge splitting test

INTRODUCTION

In most industrial applications of refractory materials, they undergo severe thermal shocks during service. To improve thermal shock resistance, the refractory materials need either a high crack initiation resistance or a high crack propagation resistance [1-2]. In many industrial applications, refractory materials with high resistance to crack propagation are used. These refractories usually show reduced brittleness, mainly due to a decrease in tensile strength [3-4]. A parameter for the quantification of the brittleness is the so called characteristic length l_{ch} introduced by Hillerborg et al. [5]:

$$l_{ch} = \frac{G_f E}{\sigma_t{}^2} \qquad (1)$$

Here, E is the Young´s modulus, σ_t is the tensile strength, and G_f is the total specific fracture energy, i.e. the consumed fracture energy divided by the single fractured cross sectional area. By reducing the tensile strength and increasing the specific fracture energy, a higher value for l_{ch} can be achieved; this indicates lower brittleness.

In magnesia spinel refractories, the addition of spinel ($MgAl_2O_4$) to magnesia (MgO) decreases the brittleness [3-4]. Due to the thermal misfit ($\alpha_{MgO} \approx 13 \cdot 10^{-6}$ K^{-1}, $\alpha_{MgAl2O4} \approx 9 \cdot 10^{-6}$ K^{-1}) a micro-crack network is formed during the cooling stage of the firing process (Fig. 1).

In this paper the fracture process during a wedge splitting test (WST) and in particular, the development of the fracture process zone (FPZ) is investigated for a magnesia and a magnesia spinel material. A short overview for chemical composition and selected physical properties is given in table 1.

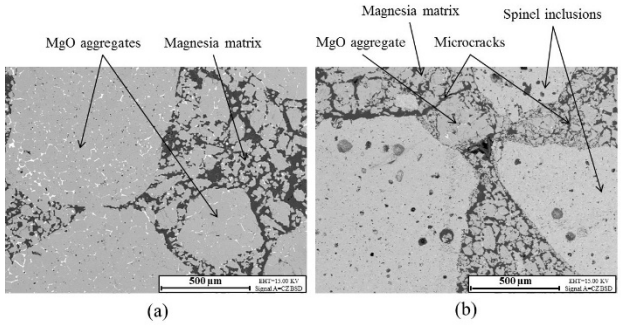

Fig. 1: Backscattered scanning electron microscopical image showing (a) magnesia and (b) magnesia spinel

Tab. 1: Chemical composition and selected properties of magnesia (M) and magnesia spinel (MA)

	MgO[%]	Al_2O_3[%]	Fe_2O_3[%]	CaO[%]	SiO_2[%]
M	97.0	0.1	0.2	1.9	0.6
MA	87.9	10.5	0.5	0.8	0.3
	Bulk density [g/cm^3]	Open porosity [vol. %]	Young's modulus E [GPa]		
M	3.02	15	105.5		
MA	2.95	16	20		

LABORATORY EXPERIMENTS

The wedge splitting test (WST) according to Tschegg [6] has been widely used to identify the fracture mechanical properties of a variety of materials, e.g. refractories, concrete or wood. The main advantages are the high ratio of crack surface to sample volume and the reduction of the strain energy due to the action of the wedge [7]. The experimental set-up applied for the investigations with DIC is shown in Fig. 2.

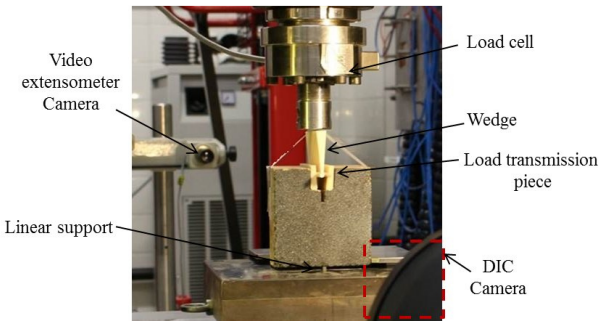

Fig. 2: Testing setup for the wedge splitting test with DIC

The specimen size used in this work is 100 mm×100 mm×75 mm. The initial notch length a_0 equals to 12 mm and the wedge angle β is 10°. The WST was performed displacement controlled with a loading rate of 0.5 mm/min. The displacement in horizontal direction was determined by a video extensometer measurement. The vertical force (F_V) is measured and the horizontal force (F_H) is calculated from F_V using Eq. (2):

$$F_H = \frac{F_V}{2\tan(\beta/2)} \qquad (2)$$

The fracture mechanical parameters of refractories, including the specific fracture energy (G_f') and the nominal notch tensile strength (σ_{NT}) can be determined from the measured load-displacement curve:

$$G_f' = \frac{1}{A}\int_0^{\delta} F_H \, d\delta_H \quad (3)$$

$$\sigma_{NT} = \frac{F_{H,max}}{bh}\left(1 + \frac{6y}{h}\right) \quad (4)$$

The specific fracture energy G_f' equals to the area under the load-displacement curve divided by the ligament area A during stable crack propagation, δ_H is the horizontal displacement, and δ is the horizontal displacement at 15% of the maximum load. In Eq. (4), $F_{H,max}$ is the maximum horizontal load, b and h are the width and the height of the ligament respectively and y is the vertical distance from the load vector to the center of the ligament.

Digital image correlation

The 2D digital image correlation technique (DIC), which was introduced by Peters et al. [8] in 1982, is a non-contact full-field measurement method. The surface displacement is obtained by tracking homologous points on the specimen surface at different loading stages. The successive digital images of the same specimen at different mechanical states are taken by a CCD or CMOS camera and are generated in a microchip segmented into a certain number of individual light-sensitive cells, so-called pixels. A random distribution of gray level, which could be the nature texture of the material surface or an artificially paint, is required for the DIC evaluation. Due to the random pattern at the specimen surface, each pixel of the image stores a certain gray level value ranging from 0 to 255. A single gray level value is not a unique signature, so the neighbor pixels are involved. A collection of pixels is called subset. The correlation algorithm locates a subset in the reference image and searches the same subset in the images of the deformed state. A step size, which is the distance between the center points of two consecutive subsets, refers to the density of the homologous points. The strain field can be calculated from the displacement field based on the strain window algorithm [9].

A CMOS camera with a resolution of 5184×3456 pixels^2 was used to acquire the images of the surface successively during the entire WST. The scale factor is 0.03 mm/pixel. A speckle pattern of white spots on a black opaque layer is applied on the specimen surface to increase the contrast and to create a random distribution of gray level. The image acquisition frequency was one image for every two seconds. At least ten images in an unloaded state, which are used to evaluate the scatter caused by the numerical correlation and interpolation algorithms uncertainty and image distortion, were taken for every test. The DIC evaluation was performed with the MatchID DIC-2D software developed by the University of Leuven [10]. A subset size of 32×32 pixels^2, a step size of 8 pixels, and a strain window size of 15×15 pixel^2 were chosen for the DIC evaluation.

RESULTS

The results part includes on the one hand the mechanical testing results gained from the force and displacement measurement and on the other hand, the evaluations based on the DIC to determine the FPZ.

Mechanical testing

Fig. 3 shows a typical result from a wedge splitting test for both, magnesia and magnesia spinel. The steeper initial slope for magnesia is a consequence of the five times higher Young's modulus compared to magnesia spinel. Furthermore, the maximum force is higher for magnesia while magnesia spinel shows its maximum at a higher vertical displacement. Magnesia spinel exhibits a longer post-peak region compared to pure magnesia. Table 2 gives some important values determined from the mechanical testing results. The tensile strength σ_t and the specific fracture energy G_f are not evaluated directly form the test results but were determined from an inverse evaluation as proposed by Jin et. al. [11]. As expected, the magnesia spinel material exhibits a significantly reduced brittleness, indicated by a significant increase of the characteristic length l_{ch}. As can be seen from table 2 the reduction in brittleness comes mainly from a decrease in strength while the increase in fracture energy is a minor contribution.

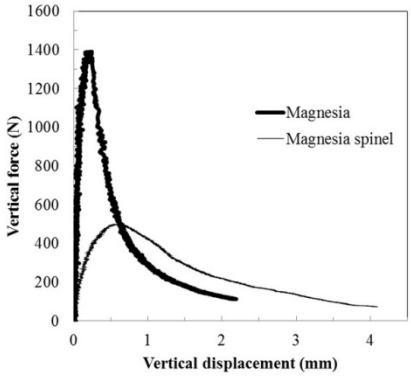

Fig. 3: Typical results for a WST for magnesia and magnesia spinel

Tab. 2: Relevant mechanical parameters for magnesia (M) and magnesia spinel (MA)

	$F_{V,max}$ [N]	σ_{NT} [MPa]	σ_t [MPa]	G_f [N/m]	l_{ch} [mm]
M	1389	11.1	7.8	211	366
MA	499	4	2.1	253	1147

Determination of the fracture process zone

The strains determined from DIC are an indicator for the definition of the fracture process zone (FPZ). Fig. 4 shows the results for selected loading stages. It is seen on the first view that for magnesia spinel a considerable process zone is formed while the magnesia material shows no pronounced FPZ. Furthermore, first occurrence of the FPZ for magnesia spinel is detected before reaching the peak load in the WST, while maximum load and initiation of the fracture process zone coincides for magnesia.

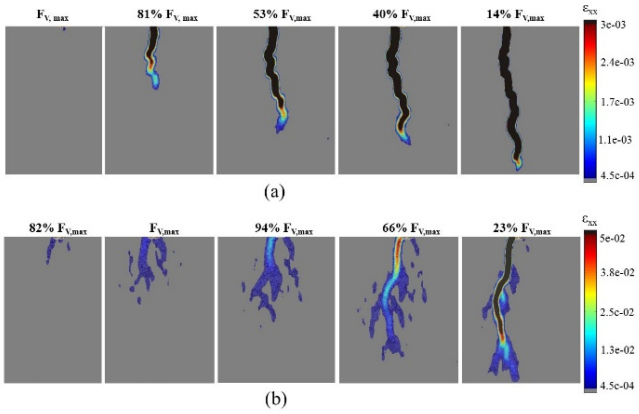

Fig. 4: Results from the digital image correlation for magnesia (a) and magnesia spinel (b)

The FPZ is defined as the area where the strain is between an upper and a lower limit. The lower limit is defined from the scatter of the DIC method. For this reason, ten pictures from an unloaded sample were evaluated. Resulting strains are due to the scatter of the method. From this scatter, a threshold of $4.5 \cdot 10^{-4}$ was obtained. The fracture process causes the strain values exceeding this lower limit. Furthermore, it should be mentioned that this lower limit is larger than the ultimate elastic strain calculated by the ratio of σ_t/E ($1.1 \cdot 10^{-4}$ for magnesia spinel, $7.4 \cdot 10^{-5}$ for magnesia). This means that pure elastic deformations are not visible in the DIC results, but not all non-elastic deformations are detected.

The upper limit of strain defines the transition between FPZ and macro-crack, i.e. the minimum strain where no interaction

between the crack faces is expected. This value was determined from the development of the FPZ. Therefore, the length L_m and width W_m of the FPZ are evaluated. An example for magnesia spinel is given in Fig. 5.

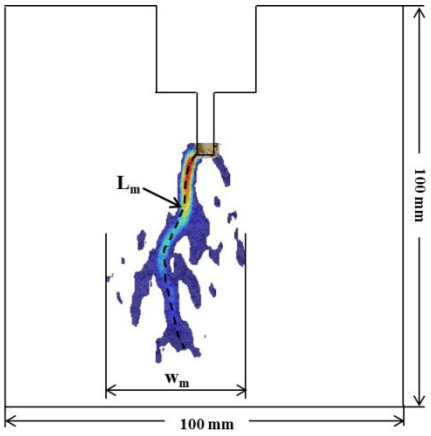

Fig. 5: Definition of width W_m and length L_m of the localized zone

The L_m and W_m were determined for several loading stages and plotted over the crack mouth opening displacement (CMOD) (Fig. 6).

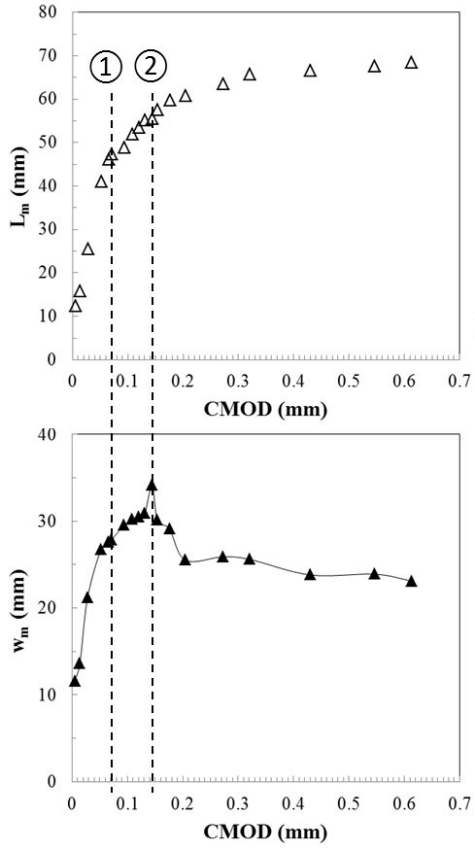

Fig. 6: L_m and W_m over the crack mouth displacement (CMOD) for magnesia spinel

The highest slope and the development of the main part of the FPZ are happening until the CMOD reaches 0.07 mm. This CMOD is marked with a dashed line and a "1" in Fig. 6. Above 0.07 mm the increase is small and W_m reaches a maximum at a CMOD of 0.144 mm. This maximum at 0.144 mm indicates the onset of the macro-crack and is also marked with dashed line and a "2" in Fig. 6. The propagation of the macro-crack unloads the surrounding material and results in a decrease in W_m. The CMOD of 0.144 mm is reached in the post peak region at a load that equals 66% of the peak load. This means that the critical strain component ε^{cr} in X-direction of magnesia spinel is 0.05. In literature, this quantity is called the tensile strain capacity [12]. Now it is possible do define the FPZ which is between $4.5 \cdot 10^{-4}$ and $5 \cdot 10^{-2}$ for magnesia spinel. Strains higher than $5 \cdot 10^{-2}$ indicate the macro-crack. According to the data shown in Fig. 6, the fracture process consists of two stages. The first stage includes the initiation and development of new micro-cracks, and the propagation of already existing micro-cracks in the virgin material i.e. the formation of a large part of the FPZ. This is already consuming a great share of the work of fracture. The second stage is characterised by the initiation and propagation of the macro-crack. More details about evaluation method and results are shown elsewhere [13].

For pure magnesia, it was assumed that the macro-crack initializes at the peak load. At the peak load a critical strain ε^{cr} of $3 \cdot 10^{-3}$ was observed. The black areas in Fig. 4 show the macro-crack where the strain is higher than $5 \cdot 10^{-2}$ for magnesia spinel and higher than $3 \cdot 10^{-3}$ for magnesia.

Development of the fracture process zone

Figure 7 illustrates the development of the FPZ for both materials. Therefor the localized zone length L_m and the macro-crack length a are plotted over the CMOD.

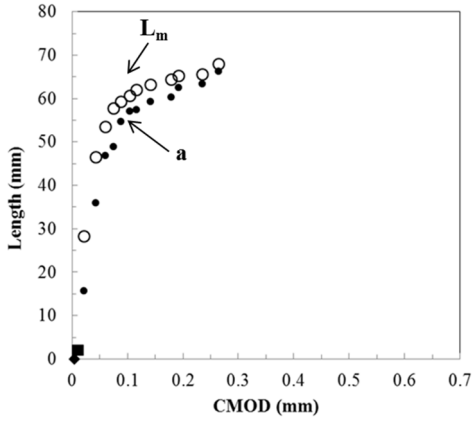

(a)

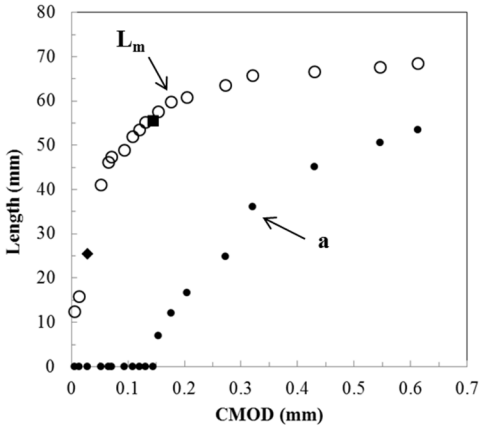

(b)

Fig. 7: Localized length L_m and crack length a over CMOD for magnesia (a) and magnesia spinel (b). (◆ maximum load, ■ onset of macro-crack)

The difference between them is the length of the FPZ. In general, the magnesia material develops a much smaller FPZ compared to the magnesia spinel. For magnesia L_m and a increase at low CMOD values. Magnesia spinel shows the formation of the FPZ only until a CMOD from 0.144 mm, but no macro-crack. At this CMOD of 0.144 mm magnesia shows already a macro-crack length of more than 55 mm.

Furthermore, the maximum CMOD is much higher for magnesia spinel. With the propagation of the macro-crack the size of the FPZ decreases. At the end of the test, the FPZ tip reaches the

compressive zone at the bottom of the testing sample. The crack propagation slows down and the FPZ decreases.

SUMMARY

The fracture mechanical behavior of industrially produced magnesia and magnesia spinel refractories was studied by wedge splitting testing and recording the fracture process with digital image correlation. In contrast to the magnesia material, magnesia spinel exhibits already in the virgin state micro-cracks initiated at the cooling stage at the end of the production process. The micro-cracks support crack branching and the formation of a fracture process zone (FPZ), and consequently, increase the energy consuming volume. The mechanical properties determined from the wedge splitting test indicate a reduction in tensile strength and an increase in fracture energy. The development of the fracture process zone in the magnesia spinel material is rather energy consuming due to effects like friction between the crack faces and grain bridging. The microstructure of magnesia spinel characterized by pre-existing micro-cracks increases the strain bearing capacity, which improves the thermal shock resistance. For magnesia, a pronounced fracture process zone could not be detected. Macro-crack propagation occurs when reaching the maximum load. For magnesia spinel, the FPZ development starts in the pre-peak region.

The fracture process for magnesia spinel can be split in two parts. First, a FPZ develops. Afterwards, a macro-crack initiates. The transition is indicated by a decrease of the FPZ width caused by the closure of the micro-cracks and propagation of the macro-crack. The initiation of the macro-crack is in the post-peak region for magnesia spinel when the load has already decreased to 66% of the maximum value. The fracture process zone of magnesia spinel contributes to the large post-peak region, stable crack propagation and high strain tolerance before failure.

ACKNOWLEDGEMENTS

Financial support by the Austrian Federal Government (in particular from Bundesministerium für Verkehr, Innovation und Technologie and Bundesministerium für Wissenschaft, Forschung und Wirtschaft) represented by Österreichische Forschungsförderungsgesellschaft mbH and the Styrian and the Tyrolean Provincial Government, represented by Steirische Wirtschaftsförderungsgesellschaft mbH and Standortagentur Tirol, within the framework of the COMET Funding Programme is gratefully acknowledged (K2 MPPE project A4.21).

REFERENCES

[1] Kingery WD. Factors affecting thermal stress resistance of ceramic materials. J. Am. Ceram. Soc, 1955; 38(1):3–15.

[2] Hasselman DPH. Unified theory of thermal shock fracture initiation and crack propagation in brittle ceramics. J. Am. Ceram. Soc. 1969; 52(11):600–604.

[3] Harmuth H, Rieder K, Krobath M, Tschegg E. Investigation of the nonlinear fracture behaviour of ordinary ceramic refractory materials. Mat. Sci. Eng. A-Struct. 1996; 214(1):53–61.

[4] Harmuth H, Tschegg EK. A fracture mechanics approach for the development of refractory materials with reduced brittleness. Fatigue Fract. Eng. Mater. Struct. 1997; 20(11):1585–1603.

[5] Hillerborg A, Modéer M., Petersson PE.. Analysis of crack formation and crack growth in concrete by means of fracture mechanics and finite elements. Cem. Concr. Res. 1976; 6(6):773–781.

[6] Tschegg EK. Equipment and appropriate specimen shape for tests to measure fracture values. Patent AT-390328; 1986.

[7] Harmuth H. Stability of crack propagation associated with fracture energy determined by wedge splitting specimen, Theor. Appl. Fract. Mech. 1995; 23(1):103–108.

[8] Peters WH, Ranson WF. Digital imaging techniques in experimental stress analysis. Optical engineering, 1982; 21(3):427.

[9] Lava P, Cooreman S, Debruyne D. Study of systematic errors in strain fields obtained via DIC using heterogeneous deformation generated by plastic FEA. Optics and Lasers in Engineering, 2010; 48(4):457-468.

[10] MatchID 2D; User´s manual, version 2016.1.

[11] Jin S, Gruber D, Harmuth H. Determination of Young's modulus, fracture energy and tensile strength of refractories by inverse estimation of a wedge splitting procedure. Eng. Frac. Mech. 2014; 116: 228-236.

[12] Swaddiwudhipong S, Lu HR, Wee T H. Direct tension test and tensile strain capacity of concrete at early age. Cem. Concr. Res. 2013; 33(12):2077-2084.

[13] Dai Y, Gruber D, Harmuth H. Observation and quantification of the fracture process zone for two magnesia refractories with different brittleness, J Eur Ceram Soc 2017; 37(6):2521-2529.